

**Two models for  
absorption by coloured  
dissolved organic matter  
(CDOM)**

OCEANOLOGIA, 44 (2), 2002.  
pp. 209–241.

© 2002, by Institute of  
Oceanology PAS.

**KEYWORDS**  
CDOM  
Gelbstoff  
Ocean colour  
UV absorption

JILL N. SCHWARZ\*  
Remote Sensing Technology Institute,  
German Aerospace Centre,  
Rutherfordstr. 2,  
12489 Berlin, Germany;  
e-mail: jschwarz@awi-bremerhaven.de

PIOTR KOWALCZUK &  
SŁAWOMIR KACZMAREK  
Institute of Oceanology, PAS,  
Powstańców Warszawy 55,  
81–712 Sopot,  
Poland, P.O. Box 68

GLENN F. COTA  
Center for Coastal Physical  
Oceanography,  
Old Dominion University  
768W 52nd Street,  
Norfolk, VA 23508, USA

B. GREG MITCHELL & MATI KAHRU  
Scripps Institution of Oceanography,  
9500 Gilman Dr., La Jolla,  
CA 92093–0218, USA

FRANCISCO P. CHAVEZ  
Monterey Bay Aquarium  
Research Institute,  
7700 Sandholdt Road, Moss Landing,  
CA 95039–9644, USA

ALEX CUNNINGHAM & DAVID MCKEE  
Dept. Physics & Applied Physics,  
University of Strathclyde,  
107 Rottenrow, Glasgow, G4 0NG, U.K.

PETER GEGE  
Remote Sensing Technology Institute,  
German Aerospace Centre,  
Oberpfaffenhofen,  
82234 Wessling, Germany

MOTOAKI KISHINO  
RIKEN- The Institute of  
Physical and Chemical Research,  
2–1 Hirosawa, Wako-shi,  
Saitama, 351–0198, Japan

DAVID A. PHINNEY  
Bigelow Laboratory for  
Ocean Sciences,  
180 McKown Point Road,  
P.O. Box 475,  
West Boothbay Harbor,  
ME 04575, USA

ROBIN RAINE  
Martin Ryan Marine Science Institute,  
National University of Ireland,  
Galway, Ireland

---

\*Now at Alfred Wegener Institute for  
Polar & Marine Research, Postfach 12 0161,  
27515 Bremerhaven, Germany

## Abstract

The standard exponential model for CDOM absorption has been applied to data from diverse waters. Absorption at 440 nm ( $a_{g440}$ ) ranged between close to zero and  $10 \text{ m}^{-1}$ , and the slope of the semilogarithmic absorption spectrum over a minimum range of 400 to 440 nm ( $s_{440}$ ) ranged between  $< 0.01$  and  $0.04 \text{ nm}^{-1}$ . No relationship was found between  $a_{g440}$  or  $s_{440}$  and salinity. Except in the southern Baltic,  $s_{440}$  was found to have a broad distribution ( $0.0165 \pm 0.0035$ ), suggesting that it should be introduced as an additional variable in bio-optical models when  $a_{g440}$  is large. An alternative model for CDOM absorption was applied to available high quality UV-visible absorption spectra from the Wisła river (Poland). This model assumes that the CDOM absorption spectrum comprises distinct Gaussian absorption bands in the UV, similar to those of benzene. Five bands were fit to the data. The mean central energy of all bands was higher in early summer (E  $\sim 7.2$ , 6.6, 6.4, 6.2 and 5.5 eV or 172, 188, 194, 200 and 226 nm) than in winter. The higher energy bands were found to decay in both height and width with increasing salinity, while lower energy bands broadened with increasing salinity.  $s_{440}$  was found to be correlated with shape parameters of the bands centred at 6.4 and 5.5 eV. While the exponential model is convenient for optical modelling and remote sensing applications, these results suggest that the Gaussian model offers a deeper understanding of chemical interactions affecting CDOM molecular structure.

## 1. Introduction

The interpretation of remotely sensed images of turbid coastal waters requires that signals from non-covarying constituents be deconvolved. Many approaches to this problem can be found in the literature: empirical algorithms similar to those developed for case I water (O'Reilly et al. 1998) can be adapted to a given case II region using *in situ* data (Tassan 1994, for example), large regional databases of inherent optical properties and corresponding water reflectance measurements can be used together with neural networks (Schiller & Doerffer 1999, Gross et al. 2000) or other optimisation routines (Doerffer & Fischer 1994). Alternatively, optical models can be developed and inverted to yield inherent optical properties (Garver & Siegel 1997, Lee et al. 1998, Stramska et al. 2000) or concentrations (Krawczyk et al. 1999, Carder et al. 1999) of substances in the water from reflectance measurements. The latter technique requires a suitable parametrisation of the optically active constituents and their optical properties. Under practical constraints, *in situ* measurements are generally limited to phytoplankton pigment concentration, inorganic sediments and coloured dissolved organic matter (CDOM, also known as gelbstoff, gilvin or yellow substances). This paper focuses on absorption by CDOM.

CDOM comprises a vast array of molecules of varying size which absorb strongly in the UV and blue. The precise chemical composition of dissolved substances is difficult to ascertain (Spitzzy & Ittekkot 1986,

Findlay & Sinsabaugh 1999). While initially seen as a disturbance to chlorophyll *a* satellite algorithms, CDOM is an important bio-optical parameter, representing a fraction of the large dissolved organic carbon (DOC) reservoir (Hedges et al. 2000), which affects productivity by modifying availability of both nutrients (McCarthy et al. 1997, Carpenter et al. 1998) and light (Kirk 1994, Neale et al. 1998). Given the variability and complexity of the molecular composition of DOC, a universal carbon-specific absorption coefficient is not expected, and has not been found (Stewart & Wetzel 1981, Blough et al. 1993, Mopper et al. 1996), although in the water processing industry monitoring of DOC concentrations using a single optical measurement in the UV is standard (Korshin et al. 1997), and seasonal, location-specific coefficients were found by Nyquist (1979) and Ferrari et al. (1996) in the southern Baltic.

Absorption by CDOM has been described using an exponential curve of the form:

$$a_g(\lambda) = a_g(\lambda_o) \exp\{-s(\lambda - \lambda_o)\}, \quad (1)$$

where  $\lambda_o$  is a reference wavelength and  $s$  is the slope of the semilogarithmic absorption curve (Jerlov 1957, Kirk 1994, for example).  $s$  is usually taken to be constant, with a value of  $0.014 \text{ nm}^{-1}$  (Bricaud et al. 1981). Equation (1) is appropriate for the UV-A/B/visible wavelengths and provides a useful parametrisation for modelling; however, the slope parameter  $s$  has been found to vary both geographically (Bricaud et al. 1981) and temporally (Kowalczyk 1999), and is also dependent on the wavelength range over which it is calculated (Bricaud et al. 1981, Carder et al. 1989, Højerslev & Aas 2001). This can be seen in Fig. 1, which shows the first derivative of the semilogarithmic CDOM absorption curve (i.e. the slope spectrum), for a sample from the Wisła river mouth in the southern Baltic.

In this case, calculating the slope over a broad wavelength range with  $\lambda_{\min} \gtrsim 300 \text{ nm}$  gives a good estimate of the slope (e.g.  $0.01923 \text{ c.f. } 0.01919 \text{ nm}^{-1}$  for 300–400 and 400–500 nm respectively); however, limiting the calculation to 2 wavelengths or to a narrow wavelength range could lead to higher errors. Despite comparatively strong absorption by this sample ( $a_g[440] = 0.9 \text{ m}^{-1}$ ), the measurement, made in a 5 cm cuvette, shows the influence of high frequency noise already in the UV. Such effects are, of course, instrument-dependent, but it is worth noting that only high quality, photo-multiplier-based spectrophotometers are capable of measuring throughout the UV-visible domain, using a single cuvette length, without compromising instrument linearity in the far UV or the signal to noise ratio (SNR) in the visible.

In selecting the reference wavelength  $\lambda_o$ , various authors have chosen values in the UV and visible domains according to the focus of the study.

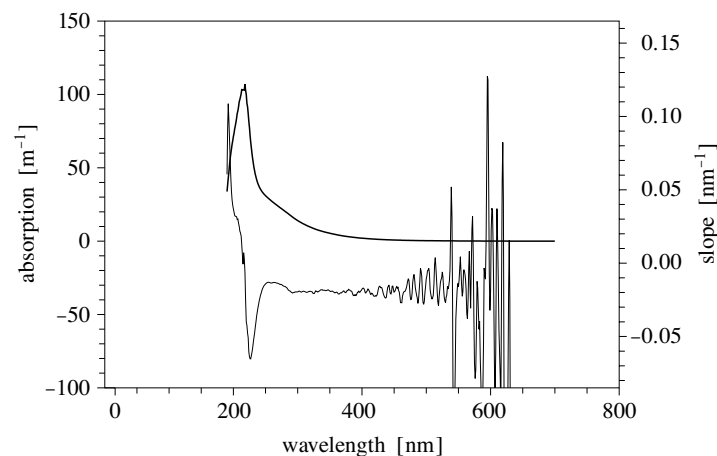


**Fig. 1.** Absorption by CDOM from surface waters at the Wisła river mouth, 18 February 1995,  $0.47 \mu\text{m}$  and  $0.2 \mu\text{m}$  filtered (bold curve, left axis), and the slope spectrum of the semilogarithmic absorption curve (thin curve, right axis)

Consideration of the SNR in open ocean waters, together with interest in the role played by CDOM in mitigating UV light levels in natural waters, has led to the use of 350 nm or lower (Højerslev & Aas 2001). Remote-sensing studies in which the competition of CDOM with phytoplankton pigments in absorption in the blue is important often employ 440 nm (Carder et al. 1989, Nelson et al. 1998, Bowers et al. 2000), and this wavelength was chosen here for the same reasons. The slope of the semilogarithmic absorption curve is henceforth calculated over a minimum range of 400 to 440 nm and referred to as  $s_{440}$  in this text, while ‘S’ denotes salinity.

The upper curve in Fig. 1 is the absorption curve itself for the visible and UV range (190 to 700 nm). It can be seen that eq. (1) is no longer useful in the UV-C range ( $\lambda \lesssim 280 \text{ nm}$ ) and slopes calculated in this region will not be applicable to the visible domain (see also Kalle 1966, Warnock et al. 1999 and Moran et al. 2000, for example). A shoulder is observed at  $\sim 260 \text{ nm}$ , as well as a peak at  $\sim 200 \text{ nm}$  (Gege 2000). Korshin et al. (1997) postulated that this absorption envelope comprises several Gaussian absorption bands, and suggested the first three electronic transitions of benzene as the basis for this model. Benzene is the aromatic ring structure which forms a part of much humic matter (Kirk 1994), and the absorption bands corresponding to the first 3 transitions occur at 6.9, 6.1 and 4.9 eV (180, 203 and 253 nm respectively, where energy in eV =  $1240/\text{wavelength in nm}$ ). Independently, Gege (2000) applied a Gaussian band fitting routine to CDOM samples from Lake Constance (Germany) and found 3 bands centred on 205, 233 and 251 nm. As noted by Korshin et al. (1997), the energy levels at which

absorption peaks are found are affected by substitution on the benzene ring. The two lower energy bands (203 and 253 nm for benzene) are in fact subject to quantum mechanical prohibition so that only when substitutions occur will absorption be observed at energies in these ranges. Further, higher molecular weight (HMW) molecules would be expected to support more functional groups attached to aromatic ring structures, resulting in a greater number of modified energy levels, and broader or split absorption peaks. The results of Gege (2000) thus support the physically-based model of Korshin et al. (1997).

We may therefore use UV-vis CDOM absorption data for two distinct purposes: firstly, to obtain information as to the chemical properties of the assemblage of dissolved molecules from their Gaussian absorption peaks, and secondly, to determine how CDOM affects the total water column absorption for remote sensing applications, using the exponential representation. These two aspects are precisely linked in that the relative magnitudes and widths of the Gaussian absorption peaks determine the slope in the exponential model. This paper addresses the question of whether, on a global scale, both parameters of the exponential model can be simply incorporated into bio-optical models by finding a relationship between them. We go on to apply the Gaussian model to see how the absorption bands affect the slope in the exponential model, and to discover whether the slope can be related to chemical information which might provide insight into the nature of a given water sample (Carder et al. 1989). For the first question, many datasets were available for study from the NASA Sensor Intercomparison and Merger for Biological and Interdisciplinary Oceanic Studies (SIMBIOS) Program<sup>1</sup>. For the deconvolution into Gaussian bands, however, the only available absorption spectra of sufficiently high quality from 190 to > 500 nm were from the southern Baltic, and no chemical analyses were available. We therefore examined the changes in the Gaussian absorption bands along a transect of a river plume, from freshwater to open water, where it can be assumed that chemical changes occur as the river water and seawater mix.

## 2. Characterisation of the waters studied

39 out of the 52 datasets used for this study were taken from the SeaBASS database, supported by the NASA SIMBIOS and SeaWiFS Projects. Data collection protocols were defined by the SIMBIOS Program (McClain & Fargion 1999a, b, Mitchell et al. 2000, Werdell et al. 2000, Barnes et al. 2001, Fargion & McClain 2001). Table 1 lists these datasets

---

<sup>1</sup>The SIMBIOS Program is funded by NASA under NRA-94-MPTE-04 and NRA-99-OES-09.

**Table 1.** SeaBASS datasets used in this study

No.	Cruise	P.I.	Funding	Region	n	$\lambda$ range [nm]	Method
4	AR98-03	D.A. Phinney	NOAA	Gulf of Maine	7	AC-9	
5	AR99-04	D.A. Phinney	NOAA	Gulf of Maine	17	AC-9	
6	AR98-08	D.A. Phinney	NOAA	Gulf of Maine	14	AC-9	
9	MOCE 1	C. Trees	NOAA	Monterey Bay	10	280:2:800	
10	MOCE 5	D. Clark	NOAA	Gulf of California	15	AC-9	
11	Arc00	G. Cota	NASA	Chukchi Sea	21	280:1:750	3
12	Lab00	G. Cota	NASA	Labrador Sea	7	280:1:750	3
13	GOCAL99A	R. Zaneveld	NASA	Gulf of California	31	AC-9	
14	GOCAL95	R. Zaneveld	NASA	Gulf of California	28	AC-9	
15	GOCAL98B	R. Zaneveld	NASA	Gulf of California	10	AC-9	
16	GOCAL96B	R. Zaneveld	NASA	Gulf of California	24	AC-9	
17	GOCAL99B	R. Zaneveld	NASA	Gulf of California	17	AC-9	
18	GOCAL97	R. Zaneveld	NASA	Gulf of California	27	AC-9	
20	ZonalFlux96	S.Pegau	OSU	Equatorial Pacific	11	AC-9	
21	S399	F. Chavez	MBARI/OSU	CalCofi line 67	2	AC-9	
22	AI9901	B.G.Mitchell	SIO	S. Atlantic, Indian Ocean	33	250:2:600	1
26	TBE 1982-84	M. Kishino	U. Tokyo	Tokyo Bay	46	350:5:750	6
27–30	BATS	D. Siegel	UCSB	Sargasso Sea	37	280:1:700	2
31	OK04998	K. Carder	USF	Lake Okeechobee	4	400:5:880	3
32	OK06499	K. Carder	USF	Lake Okeechobee	6	400:5:880	3
33	tt0400	K. Carder	USF	Florida Shelf	31	400:2:800	3
34	tt0498	K. Carder	NASA	Florida Shelf	28	380:1:679	3
35	tt0499	K. Carder	NASA	Florida Shelf	22	350:2:800	3
36	eh0100	K. Carder	USF	Florida Shelf	24	400:2:800	3

**Table 1.** (continued)

<b>No.</b>	<b>Cruise</b>	<b>P.I.</b>	<b>Funding</b>	<b>Region</b>	<b>n</b>	<b><math>\lambda</math> range [nm]</b>	<b>Method</b>
37	eh0300	K. Carder	USF	Florida Shelf	17	400:2:696	3
38	eh0399	K. Carder	USF	Florida Shelf	25	400:2:800	3
39	eh0799	K. Carder	USF	Florida Shelf	15	400:2:800	3
40	eh0999	K. Carder	USF	Florida Shelf	7	400:2:800	3
41	eh1199	K. Carder	USF	Florida Shelf	19	400:2:800	3
53	CLT00	G. Cota	NASA	Virginia Coast	6	280:1:750	3
54	Lab96	G. Cota	NASA	Labrador Sea	10	200:1:700	3
55	Lab97	G. Cota	NASA	Labrador Sea	15	200:1:750	3
59	cal0004	B.G. Mitchell	SIO/CalCOFI	California Coast	2	200:2:650	4
61	cal9809	B.G. Mitchell	SIO/CalCOFI	California Coast	2	250:2:600	4
63	cal9804	B.G. Mitchell	SIO/CalCOFI	California Coast	3	300:2:600	4
64	cal9802	B.G. Mitchell	SIO/CalCOFI	California Coast	1	300:2:600	4
65	cal9709	B.G. Mitchell	SIO/CalCOFI	California Coast	13	250:2:600	4
67	cal9704	B.G. Mitchell	SIO/CalCOFI	California Coast	2	300:2:600	4
68	cal9702	B.G. Mitchell	SIO/CalCOFI	California Coast	4	300:2:600	4

Notes: The dataset numbers (**No.**) are arbitrary labels. The wavelength range is given as: start wavelength:interval:stop wavelength. For Wetlabs AC-9 data, the wavelength bands are 412, 440, 488, 510, 530, 630, 650, 676 and 715 nm. For spectrophotometric data, method references are 1. Mitchell et al. (2000), 2. Nelson et al. (1998), 3. Mueller (1995), 4. CalCOFI reports: [www.calcofi.org](http://www.calcofi.org) and 6. Okami et al. (1982).

**Table 2.** Non-SeaBASS datasets used in this study

<b>No.</b>	<b>Cruise</b>	<b>P.I.</b>	<b>Funding</b>	<b>Region</b>	<b>n</b>	<b><math>\lambda</math> range [nm]</b>	<b>Method</b>
43	BiocolorIV	R. Raine	EU MAST III	SW Irish Shelf	18	250:1:700	5
44	BiocolorV	S. Sagan	EU MAST III	Gulf of Gdańsk	39	200:1:700	5
46	U.Strathclyde	A. Cunningham	U.Strathclyde	Scottish Lochs	10	400:1:550	
52	9502-Aku	J. Olszewski	IOPAN	Gulf of Gdańsk	2	190:1:700	5
42	9705-Opt	J. Olszewski	IOPAN	Gulf of Gdańsk	27	350:1:650	5
47	9805-Opt	S. Sagan	IOPAN	Gulf of Gdańsk	26	200:1:700	5
48	9809-Opt	J. Olszewski	IOPAN	Gulf of Gdańsk	19	200:1:700	5
49	2000-02-Opt	J. Olszewski	IOPAN	S. Baltic	29	200:1:700	5
50	2000-03-Opt	J. Olszewski	IOPAN	Gulf of Gdańsk	20	200:1:700	5
51	2000-05-Opt	J. Olszewski	IOPAN	S. Baltic	28	200:1:700	5
45	2000-09-Opt	J. Olszewski	IOPAN	Gulf of Gdańsk	46	200:1:700	5
70	2001-05-Opt	J. Olszewski	IOPAN	S. Baltic		190:1:700	5

The dataset numbers (**No.**) are arbitrary labels. The wavelength range is given as: start wavelength:interval:stop wavelength. Method references: 5. Kowalczyk (1999).

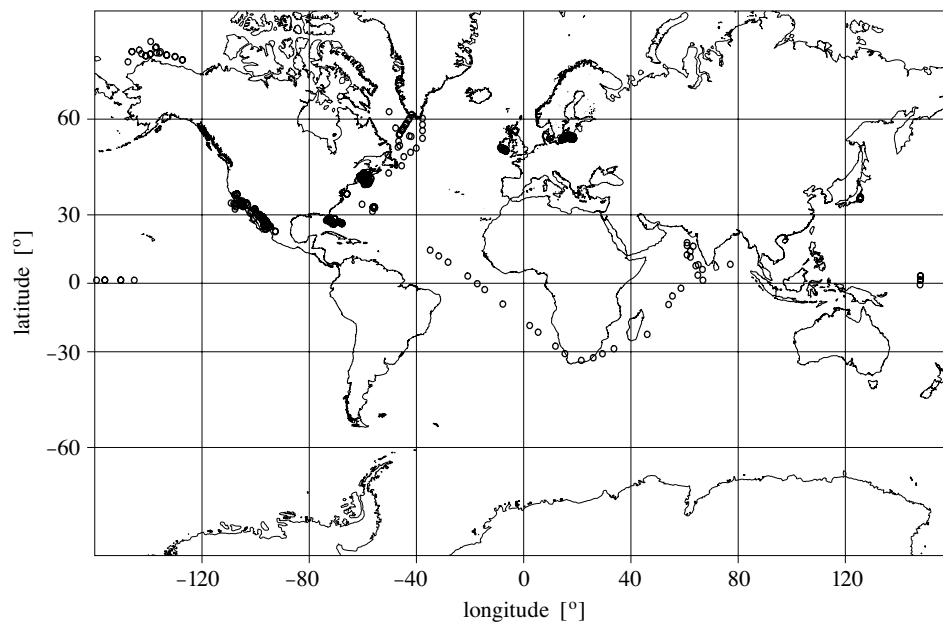


Fig. 2. Location of stations sampled ( $\circ$ )

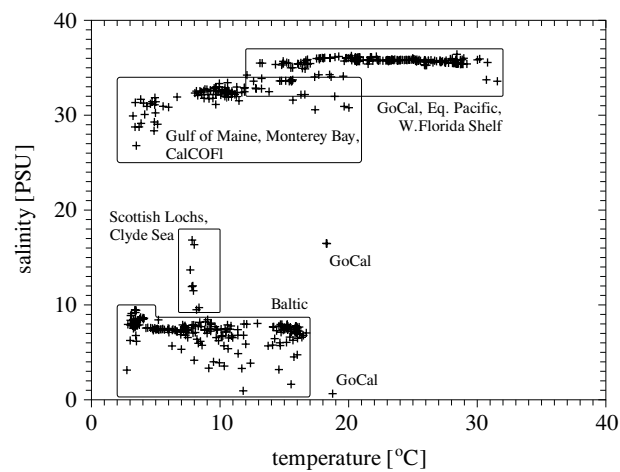


Fig. 3. Surface TS values for a subset of the study data

and indicates whether an AC-9 or a spectrophotometer was used to measure CDOM absorption for each cruise. A further 2 datasets were contributed by the EU funded Biocolor project<sup>2</sup> (Table 2). A selection of data from

<sup>2</sup>Funded under MAST III and INCO projects under contract MAS3-CT97-0085.

Scottish Lochs and the Clyde Sea were provided by A. Cunningham & D. McKee (Table 2). Finally, data were taken from 7 cruises on the Baltic (r.v. ‘Oceania’, IOPAN<sup>3</sup>) between 1995 and 2001 (Table 2). Figure 2 shows the sample locations.

Measurements of salinity, temperature and concentrations of chlorophyll and total suspended matter (TSM) were available for some datasets. Figure 3 shows the range of surface salinity and temperature conditions in which samples were taken. The spread in temperature values indicates varying diurnal as well as seasonal heating.

The variability in chlorophyll *a* and TSM is shown in Fig. 4 for those stations for which measurements were available ( $n=153$ ). Note that the chlorophyll data were obtained partly fluorometrically and partly using HPLC. The range of chlorophyll from 0.1 to  $> 40 \mu\text{g L}^{-1}$  represents oligotrophic to eutrophic conditions, as could be expected from the geographic diversity of sample locations shown in Fig. 2. Values of TSM between 0.1 and  $20 \text{ mg L}^{-1}$  reflect oceanic, coastal and river plume suspensions.

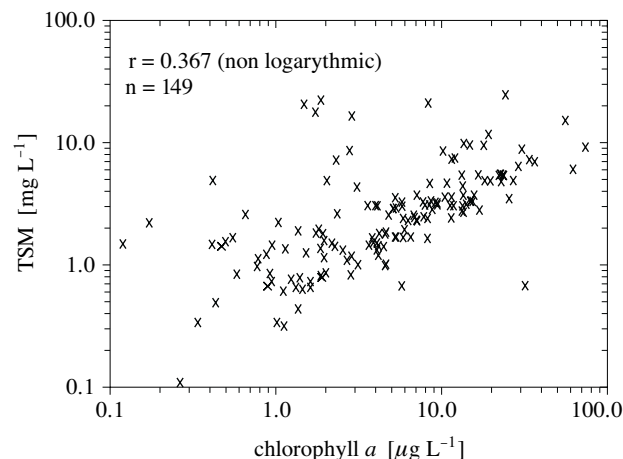


**Fig. 4.** Surface chlorophyll and TSM values for a subset of the study data

### 3. Methodology

Many of these datasets, along with the methods used, have already been published (Barnard et al. 1999, 1998, Kowalczyk 1999, Lee et al. 1999, Pegau et al. 1999, Kahru & Mitchell 2001, Loisel et al. 2001, Reynolds et al. 2001). A general description of the AC-9 and spectrophotometric determination of

<sup>3</sup>The Institute of Oceanology, Polish Academy of Sciences provided funds for this study within the framework of Statutory Research Project No. 2.3 & 2.4.

CDOM absorption is given below. Specific to this study are the calculations of  $a_g440$  and  $s440$ , also described below.

### AC-9 measurements

The AC-9 (WETLabs Inc.) measures absorption and attenuation at nine wavelengths (412, 440, 488, 510, 532, 555, 650, 676 and 715 nm), by means of twin 25 cm pathlength measurement cavities: the first is a darkened tube, in which beam attenuation is measured. The second is a reflective tube, in which absorption is measured. CDOM absorption is measured by placing a 0.2  $\mu\text{m}$  filter at the measurement cavity inlet, and attaching a pump to the outlet so that water can be drawn through the instrument at a known rate. A temperature correction is routinely applied to the data. (See also Twardowski et al. (1999), Twardowski & Donaghay (2001) and <http://www.wetlabs.com/Products/ac9/ac9man.>)

### Spectrophotometric measurements

For the spectrophotometric determination of CDOM absorption, samples are collected from discrete depths using Niskin bottles or plastic buckets and filtered on board ship. This additional handling of the samples incurs risks of contamination, for example, from components made of rubber, contact with bare skin, dust or residues on various parts of the equipment. A strict measurement protocol can be found in Mitchell et al. (2000). Earlier methods used glass fibre filters, which have been found to contaminate the samples (Bricaud et al. 1981, Mitchell et al. 2000). However, in coastal waters, filtering directly through fine pore filters as recommended in the SeaWiFS protocols results in almost immediate clogging of the filter by particulates. In this case, a well-rinsed glass fibre filter has been used to eliminate larger particles by several authors, and in coastal waters where CDOM levels are generally high, insignificant contamination has been reported (Kowalczyk 1999).

The sample collection generally proceeds with the collection of water in rinsed containers, filtration of one or two small aliquots of sample through either 0.7  $\mu\text{m}$  (GF/F – coastal) or 0.2  $\mu\text{m}$  (polycarbonate – oceanic) filters, the filtrate being firstly discarded and then used to rinse the filtrate receiving bottles, and filtration of a final aliquot, which is collected and filtered again through 0.2  $\mu\text{m}$  filters (coastal) then stored in acid-cleaned and sample-rinsed bottles in the dark until measurement. Storage of samples for longer than a day is not recommended owing to variable degradation effects. Spectrophotometric measurements of absorbance are carried out using a purified water blank, once the samples and pure water sources have been allowed to reach room temperature. Absorption is calculated as

$a(\lambda) = 2.303A(\lambda)/l$ , where  $l$  is the cuvette length in metres. The measurements used in this study were carried out using various instruments and procedures: Tables 1 and 2 include references to the published methods, where available.

### Calculation of $a_g440$ and $s440$

Measurements of CDOM absorption may be affected by scattering by small particles (Aas 2000), differences in refractive index between the ultra-pure reference water and seawater (Green & Blough 1994) and electronic noise. Bricaud et al. (1981) applied a wavelength-dependent correction for residual scattering. This approach was also used by Nelson et al. (1998); however, as discussed by Bricaud et al. (1981) and Højerslev & Aas (2001), finding a universally applicable correction is difficult without information regarding the type of particles passing through the filter. Green & Blough (1994) applied a wavelength-independent correction for refractive effects, calculated as the mean absorption between 700 and 800 nm. Similar approaches have been taken by Kowalczyk (1999) and Holder Sandvik et al. (2000). For this study, the mean of measurements at  $\lambda > 650$  nm was subtracted from the whole spectrum for all data.

A line was fitted to the semilogarithmic absorption spectrum using the linear least squares method. Values of  $a_g440$  and  $s440$  were then calculated using the fit parameters. More precisely, the fitting routine determined the constant ( $\ln a_g(\lambda = 0)$ ) and slope ( $s$ ) of the equation:

$$\ln a_g(\lambda) = \ln a_g(\lambda = 0) + s(\lambda - 0).$$

As mentioned in the introduction, the slope may be affected by instrument nonlinearity in the far-UV or by noise in the blue or green regions when the instrument detection limit is reached. The latter effect was found to be characterised by a decrease in slope. We also observed a gradual shift toward higher slopes in the 330 to 390 nm range for some spectra. The slope was calculated first for the range 350 to 500 nm. A semilogarithmic plot of the absorption curve was then examined for noise in the blue, and the upper limit of the calculation reduced accordingly. The upper and lower limits were then reduced in  $\leq 5$  nm steps until 2 successive slope calculations agreed to within 3 significant figures, and successive  $a_g440$  values predicted using the calculated  $s440$  values agreed to within 3 s.f. Data for which  $r < 0.95$  or for which no steady  $s440$  and  $a_g440$  values could be found in the range 400 to 440 nm were discarded. The effects of residual noise on the results are discussed in Section 5. Note that  $s440$  and  $a_g440$  were always calculated using wavelengths greater than 350 nm, so that effects of salts and inorganic nitrate should be minimal.

## Gaussian absorption bands

The Gaussian model places absorption bands in the UV and therefore requires absorption measurements from  $\sim 190$  to  $> 500$  nm. This placed severe restrictions on the number of datasets available for the study. Only two datasets from the Baltic included measurements over the full UV-visible range for which nonlinear instrument effects were known to have been avoided (in one case by taking measurements in both 0.5 and 5 cm cuvettes). The remaining datasets either did not start at sufficiently low wavelengths, or showed clear effects of nonlinearity at low wavelengths, or employed instruments for which no information about performance in the UV was available. Data from a transect of the Wisła river plume, S. Baltic, from February 1995 (part of which makes up dataset 52 in Table 2), and from several north-south and east-west transects in the Wisła plume, the Gulf of Gdańsk and the Gdańsk Deep in May 2001, were thus selected for analysis using Gaussian band deconvolution. Figure 9 (see page 227) shows the location of the stations for these cruises. The February 1995 dataset included only stations ZN2, P115, P110, P116, P1 and P1a. The May 2001 dataset included all stations shown except for P1a. The absorption wavelengths were converted into energy (E) according to  $E \text{ (eV)} = 1240 / \lambda \text{ (nm)}$  (Korshin et al. 1997). The **resol** program, first introduced by French et al. (1967) and used by Hoepffner & Sathyendranath (1993) and Aguirre-Gomez et al. (2001) to analyse phytoplankton absorption spectra, was used to fit 5 Gaussian bands to these spectra. The first 3 bands were located at 6.05, 5.32 and 4.94 eV (205, 233 and 251 nm respectively), after Gege (2000). Bands were added at 5.9 and 4.5 eV (210 and 276 nm) to allow for absorption band splitting. A maximum of 100 iterations were allowed for the program to converge. The central wavelength of each band could be shifted by up to 0.1 eV per iteration, and the halfwidth of each band could be adjusted by up to 0.2 eV per iteration. Weighting coefficients were used to achieve a better fit at lower wavelengths (higher energies).

## 4. Results

### Exponential model

Figure 5 shows the values of  $a_g440$  plotted against  $s440$  for all data ( $n=877$ ).  $a_g440$  values ranged from close to zero to  $10.0 \text{ m}^{-1}$ , while the slope values ranged from 0.007 to  $0.04 \text{ nm}^{-1}$ . A general tendency for higher absorption values to be associated with lower slopes is observed, with several distinct data subsets shifted toward higher  $a_g440$  values: Baltic data, represented by \*, and dataset 5 (see Table 1) from river plumes in the Gulf of Maine, plus data from the Scottish Lochs and Clyde Sea (see Table 2),

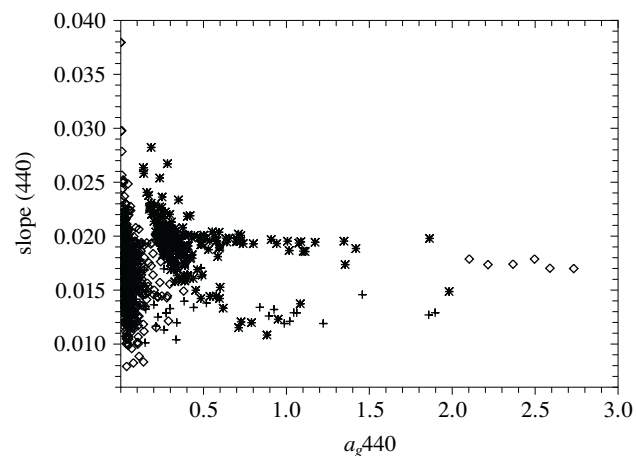


**Fig. 5.** CDOM absorption and slope values at 440 nm,  $n = 904$ . (+) values from the Gulf of Maine (datasets 1, 2, 4, 5 & 6 in Table 1 and Scottish Lochs (dataset 46, Table 2), (\*) values from the Baltic, all other data are represented by diamonds

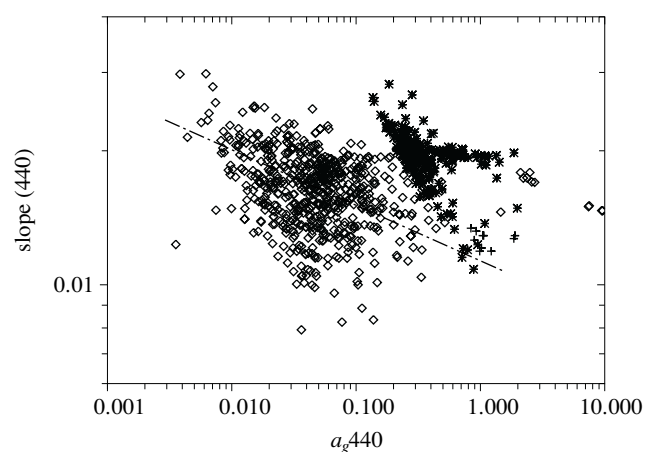


**Fig. 6.** CDOM absorption and slope values as for Fig. 5 on a natural log-log scale. The dashed line is a first-order polynomial fit to the AC-9 data (see Table 4)

shown by (+) symbols. Data from Lake Okeechobee (diamonds) represent extreme values of absorption between 2 and 10  $\text{m}^{-1}$ . Figure 6 shows the same data with logarithmically scaled axes.  $\ln(a_{g440})$  and  $\ln(s_{440})$  were weakly correlated with one another for some data subgroups (see Table 3), so that  $s_{440}$  could be calculated as a function of  $a_{g440}$  for optical modelling. First-order polynomial fits were calculated for each of the subgroups and are given in Table 4. The fit to the AC-9 subgroup, which had the best correlation coefficient ( $r = 0.48$ ), is plotted in Fig. 6.

**Table 3.** Mean and standard deviation of the absorption at 440 nm ( $a_g440$ ) and slope ( $s440$ ) for various groups of data. The number of datapoints in each subgroup is  $n$ , and  $r$  is the correlation coefficient between the natural logarithms of  $a_g440$  and  $s440$

Data Group	$a_g440$		$s440$		$a_g440:s440$	
	mean	stdev	mean	stdev	n	r
all data	0.2309	0.6438	0.01725	0.0034	877	-0.007
Baltic	0.4137	0.2694	0.0193	0.0024	236	-0.495
AC-9 data	0.0861	0.1340	0.0167	0.0033	203	-0.431
non-Baltic, non-AC9	0.1995	0.8688	0.0164	0.0035	438	-0.295
all non-Baltic	0.1636	0.7238	0.0165	0.0035	641	-0.323

**Table 4.** Polynomial fitting coefficients between  $\ln(a_g440)$  and  $\ln(s440)$  for various groups of data

Data Group	Polynomial fit to $\ln(a_g440) = m\ln(s440) + c$	
	m	c
all data	-0.00114	-4.08429
Baltic	-0.13473	-4.09303
AC-9 data	-0.12467	-4.48089
non-Baltic, non-AC9	-0.05063	-4.28151
all non-Baltic	-0.06435	-4.31660

Mean and standard deviation values of  $a_g440$  and  $s440$  are given in Table 3 for several subgroups of the data. Histograms of  $a_g440$  and  $s440$  are shown in Fig. 7 for the same data subgroups, with binsizes of  $0.1 \text{ m}^{-1}$  and  $0.01 \text{ nm}^{-1}$  respectively, and ranges of 0 to  $3 \text{ m}^{-1}$  and 0.006 to  $0.04 \text{ nm}^{-1}$ . A one-way analysis of variance between the AC-9 and spectrophotometer groups (excluding Baltic data) found no significant difference between the  $a_g440$  and  $s440$  values. Although this is not a direct comparison, these data subsets each include regions in the upper two boxes of the TS diagram (Fig. 3), suggesting that the two rather different techniques are in good agreement, even in waters with low CDOM absorption levels.

The AC-9 data show a bi-modal distribution in slope, with peaks at  $0.013$  and  $0.017 \text{ nm}^{-1}$ , while the spectrophotometer data has a single peak at  $\sim 0.016 \text{ nm}^{-1}$ . The narrowest distribution was observed in Baltic waters, centred at  $0.019 \text{ nm}^{-1}$ . The distributions of  $a_g440$  are easily separable into a higher component from the Baltic, which peaks at  $\sim 0.3 \text{ m}^{-1}$ , and a lower component from non-Baltic waters, peaking at  $< 0.1 \text{ m}^{-1}$ ; however, the exact location of the lower peak varies slightly among the groups

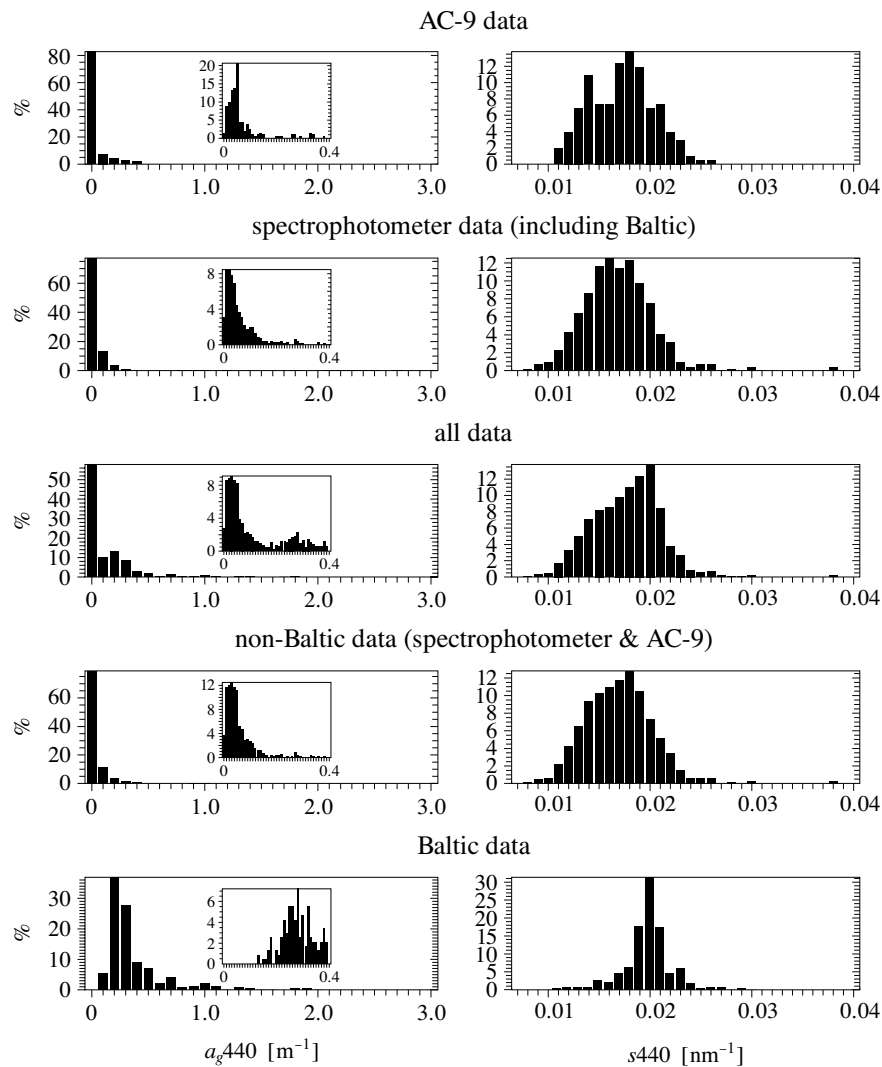


**Fig. 7.** Histograms of absorption and slope values measured for the AC-9, spectrophotometric (excluding Baltic), entire, all non-Baltic and Baltic datasets (as for Table 3)

(inset histograms have a binsize of  $0.01 \text{ m}^{-1}$  within the range  $0$  to  $0.4 \text{ m}^{-1}$ ). For the entire dataset this peak is at  $\sim 0.04 \text{ m}^{-1}$ , for the AC-9 data it is at  $\sim 0.05 \text{ m}^{-1}$ , for spectrophotometric data excluding Baltic waters at  $\sim 0.03 \text{ m}^{-1}$  and for all non-Baltic waters (AC-9 plus spectrophotometric) at  $\sim 0.04 \text{ m}^{-1}$ .

In many studies, CDOM has been found to dilute conservatively, so that salinity could be used to predict absorption levels. Figure 8

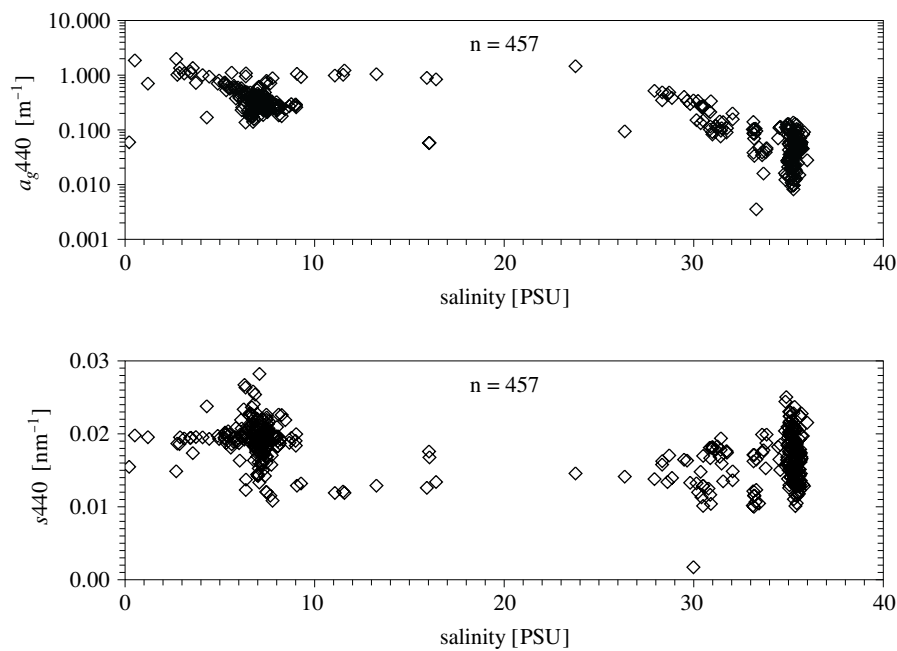


**Fig. 8.** Variability of CDOM absorption ( $a_{g440}$ ) and absorption slope ( $s_{440}$ ) with salinity

shows salinity plotted against  $a_{g440}$  and  $s_{440}$  for the 504 samples for which salinity data were available. No relationships were found between  $a_{g440}$  or  $s_{440}$  and salinity in this study.

### Gaussian model

The Gaussian band characteristics obtained for the February 1995 and May 2001 datasets are given in Table 5. Figure 9 shows the station locations for this section of the work. Absorption values for February were considerably lower than for May, both for individual bands and for total absorption at a given energy (or wavelength). The bands tended toward higher energies in May, although it should be noted that this is not a direct comparison since the May dataset included many more locations. Figure 10 shows examples of the curve-fitting results for station P110, which lies along the mean river plume transect midway through the Gulf, ZN2, approximately 1 km north of the turbulent mixing zone and Wisła South, which lies upstream in fresh water. The main absorption peak appeared at higher energies for the freshwater Wisła samples than for all other stations.

Regression of Gaussian peak characteristics for May 2001 against  $s_{440}$  showed that increases in band 5 central energy and height and decreases in band 3 width were significantly positively correlated with the slope

**Table 5.** Mean and one standard deviation Gaussian band characteristics for all stations analysed from cruises in February 1995 (n = 7) and May 2001 (n = 24)

<b>Cruise:</b>	<b>February 1995, Wisła river plume (dataset 52)</b>				
<b>Band No.</b>	1	2	3	4	5
<b>Energy [eV]</b>	6.215±.034	5.883±.091	5.790±.134	5.282±.125	4.757±.245
<b>Height [m<sup>-1</sup>]</b>	38.698±4.483	29.247±12.918	24.669±1.758	5.983±1.942	
<b>Halfwidth [eV]</b>	0.563±.062	0.350±.073	1.450±.394	2.965±.485	0.869±.322
<b>Cruise:</b>	<b>May 2001, Wisła river, Gulf of Gdańsk, S. Baltic</b>				
<b>Band No.</b>	1	2	3	4	5
<b>Energy [eV]</b>	7.225±.4766	6.554±.1782	6.403±.1822	6.161±.1901	5.450±.4486
<b>Height [m<sup>-1</sup>]</b>	1387±2340	395±194	380±217	234±146	48±56
<b>Halfwidth [eV]</b>	1.064±.433	0.718±.508	0.579±.568	0.604±.631	1.981±.601

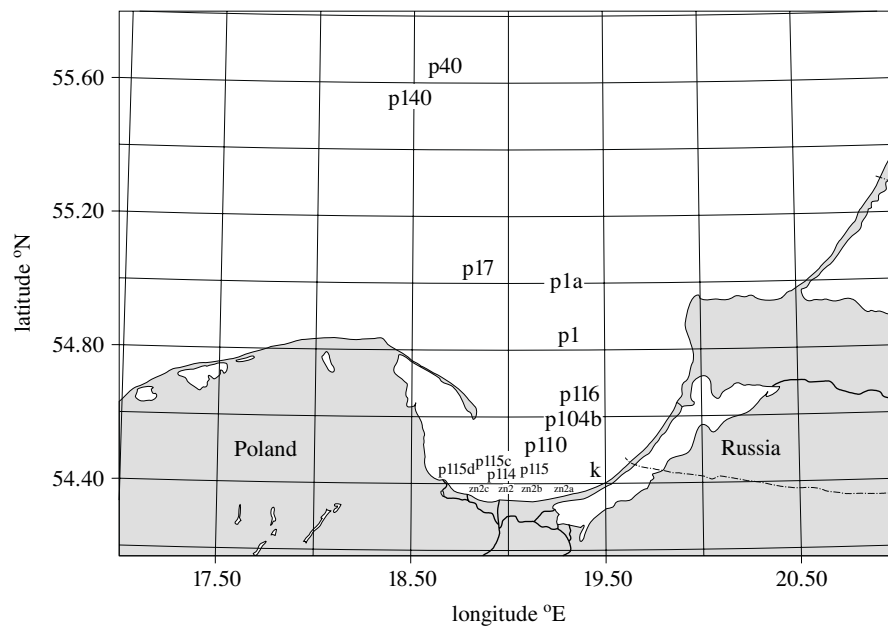


**Fig. 9.** Location of stations for the **resol** curve-fitting analysis

(the percentage variance in  $s_{440}$  values explained was 52, 49 and 27% respectively,  $n=24$ ). When multiple regressions were applied, either to the central energy, height and width of an individual band or to a given parameter for all bands, against  $s_{440}$ , significant correlation coefficients were obtained ( $r > 0.8$ ,  $n=24$ ), giving reassurance that **resol** converged to solutions which were consistent across the dataset. This analysis was not possible for the February data as absorption values were too low at  $\lambda > 400$  nm for the  $s_{440}$  calculation for all but two stations.

Of the three band characteristics found to correlate well with  $s_{440}$ , only the central energy of band 5 was found to be significantly affected by salinity and chlorophyll (see Fig. 11). SeaWiFS data for 13.5.2001 showed the Wisła plume to be flowing eastwards, close to the coast. Stations ZN2, ZN2b, ZN2a and K, lying directly in the plume, were observed to behave differently with respect to salinity and chlorophyll than other stations (Fig. 11). Regressions of salinity and chlorophyll against band 5 central energy for all stations except this subgroup resulted in correlation coefficients ( $r$ ) of 0.898 and -0.811 respectively (significant for  $\alpha = 0.01$ ,  $n = 15$ ), and a multiple regression using salinity and chlorophyll as predictor variables gave  $r = 0.903$ .

In contrast, almost all band parameters were significantly correlated with salinity during February 1995: the central energies of bands 1, 2, 3 and 5

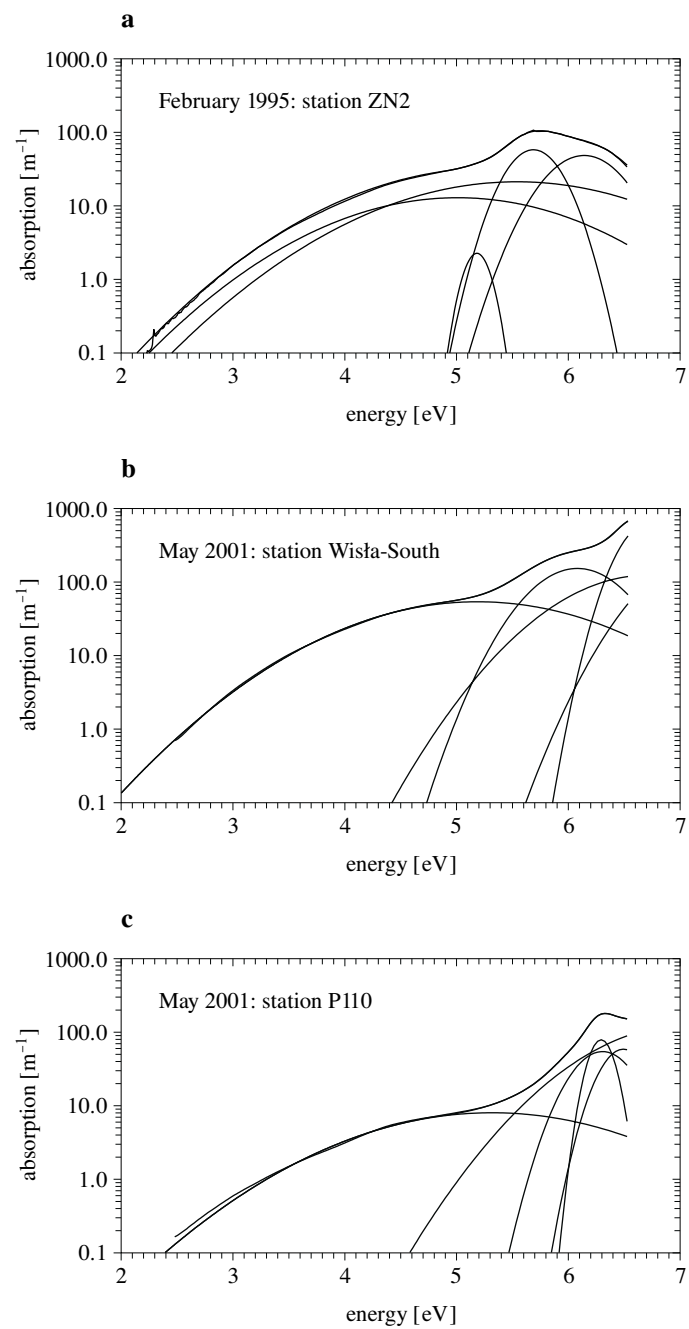


**Fig. 10.** Results of fitting 5 Gaussian bands to absorption spectra from (a) station ZN2, Feb. 1995, (b) the southern Wisła river sample, May 2001 and (c) station P110, May 2001

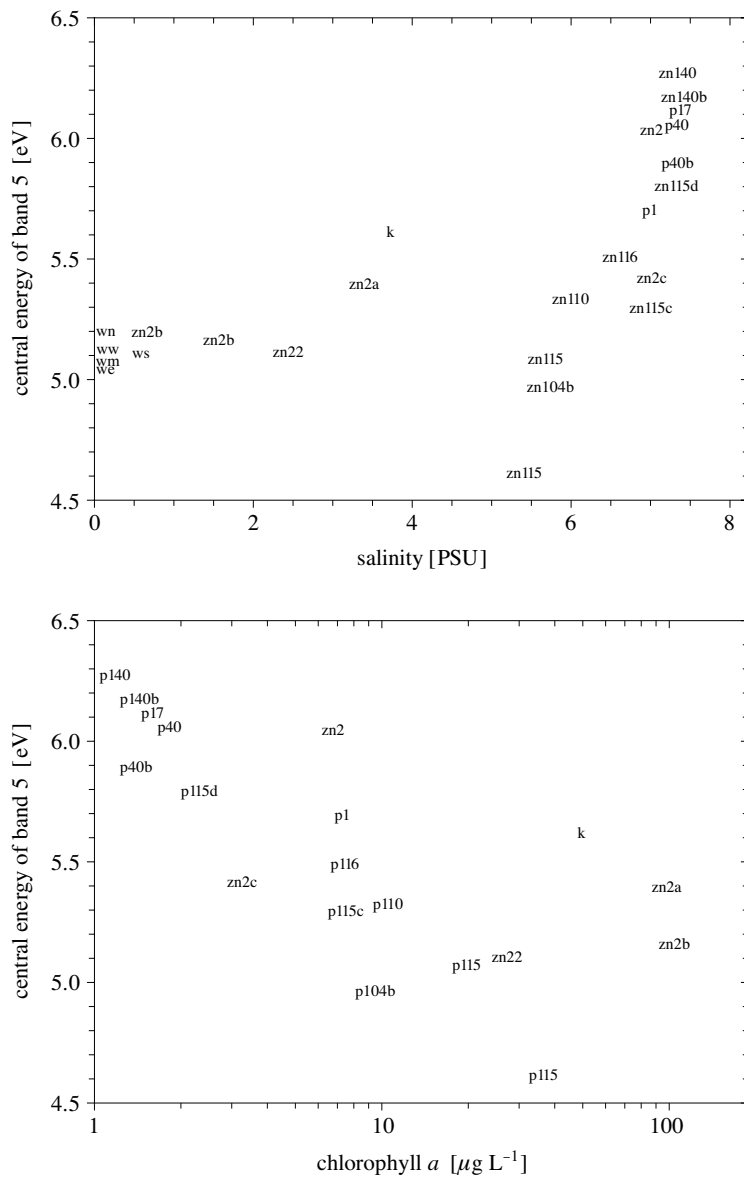


**Fig. 11.** Variation in the central energy of Gaussian band 5 with salinity and chlorophyll

were positively correlated with  $S$  ( $r > 0.95$ ,  $n = 6$ ), the heights of bands 1 and 2 were negatively correlated with  $S$  ( $r < -0.917$ ), the heights of bands 4 and 5 were positively correlated with  $S$  ( $r > 0.92$ ), the halfwidth of band 2 was negatively correlated with  $S$  ( $r = -0.932$ ), while the halfwidth of band 5 was positively correlated with  $S$  ( $r = 0.960$ ). That is, with increasing salinity,

all bands shifted to higher energies (shorter wavelengths), but the highest energy bands became shorter and narrower whereas the lower energy bands became taller and broader.

## 5. Discussion

Similar to the results of Kowalczyk (2001), statistically significant relationships were found between  $\ln(a_g440)$  and  $\ln(s440)$  for 2 subsets of the data – the AC-9 and Baltic datasets. However, at best 24% of the variance between these parameters could be explained, so that the regression relationships do not represent a useful improvement over the current practice of assuming  $s440$  to be constant. The mean  $s440$  values for all subgroups of the data were higher for the 400 to 440 nm region than the currently used value of  $0.014 \text{ nm}^{-1}$ , namely  $0.016 \text{ nm}^{-1}$  for non-Baltic waters and  $0.019 \text{ nm}^{-1}$  for the Baltic. The value of  $0.014 \text{ nm}^{-1}$  was originally found by Bricaud et al. (1981) and there are a number of differences between their methods and those used in this study. For example, GF/C filters were used together with a correction for residual scattering rather than the combination of GF/F and  $0.2 \mu\text{m}$  filters, and the slope calculations were performed over the region 375 to 500 nm for all spectra. The broad distributions of slope obtained here suggest that, since  $s440$  can not be linked to  $a_g440$ , the inclusion of  $s440$  as an additional retrieval parameter for remote sensing applications is certainly desirable when CDOM absorption is high.

No relationship was found between the coefficient of determination  $r^2$  of the semilogarithmic absorption curve and either  $a_g440$  or  $s440$ , ruling out the possibility that residual noise caused any trends toward higher or lower values. Furthermore, the range in slope values was higher when  $r^2 > 0.99$  than when  $r^2 < 0.95$ , so that it was unlikely that residual noise resulted in the broad frequency distributions for these parameters observed in Fig. 8. Another possible cause of the breadth of the distributions is variability in the sample collection and measurement techniques.

The relationship between  $\ln(a_g440)$  and  $\ln(s440)$  at higher absorption values comprised two branches, one steeper than the fit to the AC-9 data and another with similar slope but offset toward higher values of  $a_g440$  by more than one order of magnitude (Fig. 6). A closer analysis of the May 2001 dataset for the southern Baltic showed a similar distribution, with the lower branch representing samples taken from open water (P17, P40, P140 in Fig. 9). Distinctive relationships were found for these stations during May 2001, namely  $\ln(\text{chl}) \propto -\ln(a_g440)$ , and  $\ln(\text{chl}) \propto \ln(s440)$ . Contrarily for the other stations chlorophyll was found to be directly proportional to  $a_g440$  and no relationship existed between chlorophyll and  $s440$ . We conclude

that, nearshore, CDOM absorption from the Wisła plume is associated with riverine phytoplankton or new production in the nutrient-rich plume waters (Benner & Opsahl 2001), whereas  $s_{440}$  is affected by other factors, and that similar conditions may prevail in the global dataset.

The behaviour of the Gaussian peak characteristics in the Wisła plume during February, specifically the growth of the lower energy peak and the diminution of the higher energy peaks, represents sources and sinks of the different absorption bands resulting from the mixing of fresh and saline water. Without chemical analysis of the water the reactions occurring can not be identified. While inorganic nutrients and salt have been found to contribute insignificantly to CDOM absorption at near-UV and visible wavelengths (Kirk 1994), in the far UV the effects of these substances must be considered. Woźniak (1995) found that salt absorption could reach  $\sim 80\%$  of total absorption in clear natural waters (Smith & Baker 1981) in the spectral region 230 to 300 nm. That is, salt absorption is of the same order of magnitude as pure water, accounting for up to 0.01% of CDOM absorption measured in the southern Baltic, when a pure water reference is used (note that  $S \leq 7$  PSU for all samples used in the Gaussian band analysis). Rozan & Luther (2002) have developed a chromatographic technique for separating the major anions which contribute to absorption in the UV. Taking  $\text{NO}_3^-$  as an example, their maximum absorbance of  $\sim 0.2$  at 210 nm in a 1 cm cell, for a concentration of  $15 \mu\text{M}$ , corresponds to an absorbance efficiency of  $0.213 \text{ mg}^{-1} \text{ l}$  ( $15 \mu\text{M NO}_3^- \sim 0.93 \text{ mg l}^{-1}$ ). Łysiak-Pastuszek (2000) (L-P) reported maximal values of nitrate in the Gulf of Gdańsk of  $80 \text{ m Mm}^{-3}$  (L-P Fig. 2c), with multi-annual mean values of  $< 10 \text{ m Mm}^{-3}$  (L-P Table 5), respectively 4.96 and  $0.62 \text{ mg l}^{-1}$ , giving mean nitrate absorption values of  $\sim 0.13$ , maximum 1.06 absorption units. Our Wisła samples had peak absorbance values at  $\sim 200$  nm of between 35 and 52 (converted to 1 cm cell), so that nitrate could account for on average  $< 0.55\%$  of the absorbance peak, but with extreme values of 3%. A similar calculation for bromide (atomic mass 80 g, concentration in seawater at 35 PSU = 0.065 ppt by weight, Rozan & Luther report absorbance of  $\sim 1.25$  at a concentration of  $8.4 \mu\text{M}$  in a 1 cm cell) gives contributions of 10 and  $\sim 50\%$  of our maximum absorbance values at 200 nm for salinities of 1 and 7 PSU respectively. Further use of the Gaussian band analysis should thus account for inorganic molecules by subtracting the relevant spectra (after Korshin et al. 1997); however, their presence alone can not explain the discrepancy in the behaviour of Gaussian bands at different wavelengths as the Wisła water mixes in the Gulf of Gdańsk. Note that the decrease we observed in low wavelength absorption peaks with increasing salinity directly contradicts the results above calculated using the data of Rozan & Luther (2002).

Mixing of river water with saline water in river plumes and estuaries has been associated with both loss and gain in the DOC pool (Hedges & Keil 1999, Raymond & Bauer 2001). At low salinities in the Mississippi (< 10 PSU), Benner & Opsahl (2001) observed losses of DOC as well as significant loss of lignin, and noted that the HMW fraction appears to be particularly susceptible to flocculation. At very low salinity in the turbidity maximum, however, a gain in HMW DOC was observed, suggesting desorption from suspended sediments. At mid- to oceanic salinities, autochthonous production was inferred from an increase in neutral sugar concentrations. Harvey & Mannino (2001) also observed a peak in DOM (and DOC) concentrations at the turbidity maximum of the Delaware estuary system, with subsequent non-conservative decreases in DOM. The non-conservative DOM fraction was identified as HDOM (1 to 30 kDa), the second most abundant size fraction for all Delaware water samples studied, which was strongly influenced by salinity but also by TSM concentrations. HDOM was also the smallest size fraction showing evidence of prior degradation, in contrast to POM and VHDOM (> 30 kDa) which resembled living organic matter. Pempkowiak (1988) found that flocculation is responsible for the removal of between 8 and 40% of aquatic humic substances from riverine water in the Wisła river estuary, and was selective of higher molecular weight substances (> 5 kDa). The share of such molecules in the DOC composition was found to drop from 30 to 7% in the Wisła river waters. In the present study of Wisła river waters, absorption band characteristics were found to behave more conservatively in February than in May, indicating that temperature-dependent and/or seasonal processes are important for the cycling of (coloured) DOM. Thingstad et al. (1997) suggested that DOM accumulation in open waters results from imbalance between autochthonous production and microbial breakdown, and the same argument can be applied to riverine CDOM. Bacterial activity was found by Zweifel (1999) to be controlled by temperature, which would account for the seasonal differences observed for the Wisła. Another possible seasonal mechanism for DOM alteration is photo-oxidation, which would be weak in February, but stronger in May. Moran et al. (2000) found that bacterial uptake significantly affected the slope of the absorption spectrum of DOM pre-treated with UV-light, but that uptake of non-irradiated samples had no effect on the absorption spectrum.

In general, the coupling between absorption characteristics and biochemical processes is not fully understood. The association of increased MW with decreasing spectral slope follows from early studies of clay suspensions (Ghosh & Schnitzer 1979), and is frequently cited by soil scientists using

the absorbance ratio A465/A665 or A250/A365 (de Haan et al. 1983). Pages & Gadel (1990) showed that the relationship between absorption at 254 nm and the slope of the semilogarithmic absorption curve (as plotted in Fig. 8) is a function of the relationship between molecular weight and DOC:  $dMW/d[DOC]$ , where a low value of this ratio indicates DOM with a wide range of molecular DOC content and a narrow MW range. Carder et al. (1989) showed that, for the fulvic acid fraction (regarded as being LMW), the slope value is only weakly inversely related to MW, whereas the specific absorption coefficient is directly proportional to MW, and that specific absorption is inversely correlated to MW for the larger humic acids. In this case, non-conservative behaviour of CDOM absorption would arise from a change in the absorbing efficiency of the molecules, rather than from a source of DOM.

Many studies agree that MW itself is strongly influenced by pH, either because of coiling of the molecules at low pH (Ghosh & Schnitzer 1979) or because of flocculation (Patel et al. 1999) or complexing of DOM with metals (de Haan 1983, Ashley 1996). Summers & Roberts (1988) observed desorption of aquatic, terrestrial and commercial DOM from particulates with increasing pH, but only at  $pH > 10.5$ , with an associated increase in slope in the UV (240 to 400 nm) and decrease in slope in the visible (400 to 700 nm). In terms of the Gaussian model this would correspond to a narrowing and shifting of absorption bands toward higher energies, as was observed in the Wisła plume with increasing salinity. Grzybowski (2000) also found wavelength-selective effects of photolysis in Baltic waters, with an apparent absorption band between 280 and 300 nm (depending on whether the sample came from the Wisła river plume or coastal waters) which decayed during UV irradiation, with a noticeable effect after only a few hours. Such spectrally selective behaviour has not often been noted in the literature and supports Korshin et al. (1997)'s absorption band model for CDOM. On the other hand, Blough et al. (1993) observed little influence of pH or ionic strength on DOC-specific absorption values or absorption slopes of CDOM from the Orinoco river, and found conservative behaviour of DOM at low salinities ( $S < 30$  PSU).

The true effects of interplay between pH, functional group substitution on the aromatic ring, metal complexing and MW on absorption clearly require further investigation. The dynamics of riverine DOM have direct implications for the carbon cycle and estuarine  $CO_2$  production (Frankignoulle et al. (1998). Owing to great variability between different land/river systems this area is not yet fully understood (Hedges et al. 1997, Hedges

& Keil 1999), and the use of Gaussian band deconvolution of CDOM absorption represents a new application of UV spectroscopy which could provide a valuable additional tool for studies of these systems.

## 6. Conclusions

The first aim of this study was to discover whether  $a_{g440}$  and  $s440$  could be inter-related so that both parameters could be included in bio-optical models, thus reducing uncertainty in the slope,  $s440$ . Two subsets of data yielded statistically significant relationships – that measured using the AC-9 and that for the southern Baltic. Baltic waters have been found to be unique in their high CDOM absorption and require special algorithms for remote sensing (Siegel et al. 1999, Darecki et al. 2000). It was also found that the range of values of  $s440$  which should be used in forward modelling, for example, in generating look-up tables or training neural networks, is considerably narrower than in other waters, for the southern Baltic region examined here.

The further aim of this study was to apply the Gaussian model to CDOM absorption spectra from a transect along which chemical changes in the DOM could be expected, and to note the effects of changing absorption band characteristics on  $s440$ . The behaviour of the bands themselves was found to vary seasonally, but both in winter and in early summer distinctive changes in the height, location and width of the bands occurred as fresh and saline waters mixed. During winter, the higher energy bands behaved conservatively with salinity, but the lower energy bands expanded with increasing salinity, suggesting a source for low energy chemical bonds. The potential for monitoring chemical changes using visible wavebands (specifically  $s440$ ) during winter could not be explored owing to a lack of  $s440$  data for this period. During summer, the behaviour of the Gaussian bands along the river plume and in open waters in the southern Baltic was much more complex, but distinct relationships were found between band 3 and 5 parameters and  $s440$ , suggesting that a deeper understanding of the chemical changes influencing the absorption bands could improve our understanding of the variability in  $s440$ . Furthermore, if  $s440$  can be retrieved either by linking it to  $a_{g440}$  or by treating it as an additional variable, then there is potential for obtaining chemical information from remotely sensed data. However, combined chemical and UV-visible spectroscopy studies are required to provide a proper understanding of the behaviour of the Gaussian absorption bands of CDOM.

## Acknowledgments

The NASA SIMBIOS Program funded the collection of the *in situ* data from SeaBASS under NRA-94-MPTE-04 and NRA-99-OES-09, specifically Goddard Space Flight Space (GSFC) SIMBIOS contract numbers NASA-5-97132, NASA-5-97130, NASA-5-97268, NASA-5-97137, NASA-5-97134, NASA-5-97128, NASA-5-97125, and NASA-5-97129. Permission to use additional data from the SeaBASS archive was kindly given by the Optical Oceanography group at Oregon State University, David Siegel (Donald Bren School of Environmental Science & Management, University of California), Norman Nelson (Bermuda Biological Station for Research), Ken Carder, Frank Muller-Karger & Ramon Varela (University of South Florida), Dennis Clark (National Environmental Satellite, Data & Information Service), B. Greg Mitchell (Scripps Institute of Oceanography) and Chuck Trees (San Diego State University). Our thanks go to Sean Bailey and Jeremy Werdell who worked on quality control of the SeaBASS data sets, and on the design and development of the SeaBASS database, under funding from the NASA SIMBIOS Project at Goddard Space Flight Center. We would also like to thank Pete Shaw for useful discussions.

## References

- Aas E., 2000, *Spectral slope of yellow substance: problems caused by small particles*, Proc. Ocean Optics XV, Monaco, 16–20 October 2000.
- Aguirre-Gomez R., Weeks A.R., Boxall S.R., 2001, *The identification of phytoplankton pigments from absorption spectra*, Int. J. Remote Sens., 22 (2–3), 315–338.
- Ashley J. T. F., 1996, *Adsorption of Cu(II) and Zn(II) by estuarine, riverine and terrestrial humic acids*, Chemosphere, 33 (11), 2175–2187.
- Barnard A. H., Pegau W. S., Zaneveld J. R. V., 1998, *Global relationships of the inherent optical properties of the oceans*, J. Geophys. Res., 103 (C11), 24955–24968.
- Barnard A. H., Zaneveld J. R. V., Pegau W. S., 1999, *In situ determination of the remotely sensed reflectance and the absorption coefficient: closure and inversion*, Appl. Opt., 38 (24), 5108–5117.
- Barnes R., Clark D. K., Esaias W. E., Fargion G. S., Feldman G. C., McClain C. R., 2001, *Development of a consistent multi-sensor global ocean color time series*, Proc. Int. Workshop on Geo-Spatial Knowledge Processing for Natural Resource Management, University of Insubria, Varese, Italy, 28–29 June 2001, 13–28.

- Benner R., Opsahl S., 2001, *Molecular indicators of the sources and transformations of dissolved organic matter in the Mississippi river plume*, *Org. Geochem.*, 32, 597–611.
- Blough N. V., Zafiriou O. C., Bonilla J., 1993, *Optical absorption spectra of waters from the Orinoco River outflow: terrestrial input of coloured organic matter to the Caribbean*, *J. Geophys. Res.*, 98 (C2), 2271–2278.
- Bowers D. G., Harker G. E. L., Smith P. S. D., Tett P., 2000, *Optical properties of a region of freshwater influence (the Clyde Sea)*, *Estuar. Coast. Shelf Sci.*, 50, 717–726.
- Bricaud A., Morel A., Prieur L., 1981, *Absorption by dissolved organic matter of the sea (yellow substance) in the UV and visible domains*, *Limnol. Oceanogr.*, 26 (1), 43–53.
- Carder K. L., Chen F. R., Lee Z. P., Hawes S. K., Kamykowski D., 1999, *Semianalytic Moderate-Resolution Imaging Spectrometer algorithms for chlorophyll-a and absorption with bio-optical domains based on nitrate-depletion temperatures*, *J. Geophys. Res.*, 104 (C3), 5403–5421.
- Carder K. L., Steward R. G., Harvey G. R., Ortner P. B., 1989, *Marine humic and fulvic acids: their effects on remote sensing of ocean chlorophyll*, *Limnol. Oceanogr.*, 34 (1), 68–81.
- Carpenter S. R., Cole J. J., Kitchell J. F., Pace M. L., 1998, *Impact of dissolved organic carbon, phosphorus and grazing on phytoplankton biomass and production in experimental lakes*, *Limnol. Oceanogr.*, 43 (1), 73–80.
- Darecki M., Weeks A. R., Sagan S., Kaczmarek S., Kowalczyk P., 2000, *Optical characteristics of two contrasting Case 2 waters and their influence on remote sensing algorithms*, *Continental Shelf Res.*, (submitted).
- de Haan H., Werlemark G., de Boer T., 1983, *Effect of pH on molecular weight and size of fulvic acids in drainage water from peaty grassland in NW Netherlands*, *Plant. Soil*, 75, 63–73.
- Doerffer R., Fischer J., 1994, *Concentrations of chlorophyll, suspended matter and CDOM in case II waters derived from satellite Coastal Zone Color Scanner data with inverse modelling methods*, *J. Geophys. Res.-Oceans*, 99 (C4), 7457–7466.
- Fargion G. S., McClain C. R., 2001, *SIMBIOS Project 2000 Annual Report*, NASA TM 2001–209976, Greenbelt, Maryland, Goddard Space Flight Centre, 164 pp.
- Ferrari G. M., Dowell M., Grossi S., Targa C., 1996, *Relationship between the optical properties of chromophoric dissolved organic matter and total concentration of dissolved organic carbon in the southern Baltic Sea region*, *Mar. Chem.*, 55, 299–316.
- Findlay S., Sinsabaugh R. L., 1999, *Unravelling the sources and bioavailability of dissolved organic matter in lotic aquatic ecosystems*, *Mar. Freshwat. Res.*, 50, 781–790.
- Frankignoulle M., Abril G., Borges A., Bourge I., Canon C., Delille B., Libert E., Théate J.-M., 1998, *Carbon dioxide emission from European estuaries*, *Science*, 282, 434–436.

- French C. S., Brown J. S., Prager L., Lawrence M. C., 1967, *Analysis of spectra of natural chlorophyll complexes*, Carnegie Inst. Washington, Yearb., 67, 536–546.
- Garver S. A., Siegel D. A., 1997, *Inherent optical property inversion of ocean color spectra and its biogeochemical interpretation: 1. Time series from the Sargasso Sea*, J. Geophys. Res., 102 (C8), 18,607–18,625.
- Gege, P., 2000, *Gaussian model for yellow substance absorption spectra*, Proc. Ocean Optics XV, Monaco 16–20 October 2000.
- Ghosh K., Schnitzer M., 1979, *UV and visible absorption spectroscopic investigations in relation to macromolecular characteristics of humic substances*, J. Soil Sci., 30, 735–745.
- Green S. A., Blough N. V., 1994, *Optical absorption and fluorescence properties of chromophoric dissolved organic matter in natural waters*, Limnol. Oceanogr., 39 (8), 1903–1916.
- Gross L., Thiria S., Frouin R., Mitchell B. G., 2000, *Artificial neural networks for modelling the transfer function between marine reflectance and phytoplankton pigment concentration*, J. Geophys. Res., 105 (C2), 3483–3495.
- Grzybowski W., 2000, *Effect of short-term sunlight irradiation on absorbance spectra of chromophoric organic matter dissolved in coastal and riverine water*, Chemosphere, 40, 1313–1318.
- Harvey H. R., Mannino A., 2001, *The chemical composition and cycling of particulate and macromolecular dissolved organic matter in temperate estuaries as revealed by molecular organic tracers*, Org. Geochem., 32, 527–542.
- Hedges J. I., Eglinton G., Hatcher P. G., et al., 2000, *The molecularly-uncharacterised component of nonliving organic matter in natural environments*, Org. Geochem., 31, 945–958.
- Hedges J. I., Keil R. G., 1999, *Organic geochemical perspectives on estuarine processes: sorption reactions and consequences*, Mar. Chem., 65, 55–65.
- Hedges J. I., Keil R. G., Benner R., 1997, *What happens to terrestrial organic matter in the ocean?*, Org. Geochem., 27 (5/6), 195–212.
- Hoepffner N., Sathyendranath S., 1993, *Determination of the major groups of phytoplankton pigments from the absorption spectra of total particulate matter*, J. Geophys. Res.-Oceans, 98 (C12), 22789–22803.
- Højerslev N. K., Aas E., 2001, *Spectral light absorption by yellow substance in the Kattegat-Skagerrak area*, Oceanologia, 43 (1), 39–60.
- Holder Sandvik S. L., Bilski P., Pakulski J. D., Chignell C. F., Coffin R. B., 2000, *Photogeneration of singlet oxygen and free radicals in dissolved organic matter isolated from the Mississippi and Atchafalaya River plumes*, Mar. Chem., 69, 139–152.
- Jerlov N. G., 1957, *A transparency-meter for ocean water*, Tellus, 9, 229–233.
- Kahru M., Mitchell B. G., 2001, *Seasonal and nonseasonal variability of satellite-derived chlorophyll and colored dissolved organic matter concentration in the California Current*, J. Geophys. Res.-Oceans, 106 (C2), 2517–2529.

- Kalle K., 1966, *The Problem of Gelbstoff in the Sea*, Oceanogr. Mar. Biol. Ann. Rev., 4, 91–104.
- Kirk J. T. O., 1994, *Light and photosynthesis in aquatic ecosystems*, 2nd edn., Cambridge University Press, New York, 509 pp.
- Korshin G. V., Chi-Wang L., Benjamin M. M., 1997, *Monitoring the properties of natural organic matter through UV spectroscopy: a consistent theory*, Water Res., 31 (7), 1787–1795.
- Kowalczyk P., 1999, *Seasonal variability of yellow substance absorption in the surface layer of the Baltic Sea*, J. Geophys. Res., 104 (C12), 30,047–30,058.
- Kowalczyk P., 2001, *Yellow substance absorption in the Baltic Sea*, PhD Thesis, Inst. Oceanol. PAN, Sopot, 141 pp., (in Polish).
- Krawczyk H., Neumann A., Hetscher M., 1999, *Principal Component Inversion – Physical and mathematical background*, Proc. 3rd Int. Workshop on MOS-IRS and Ocean Colour, Berlin, 21–23 April 1999: Wissenschaft und Technik Verlag.
- Lee Z. P., Carder K. L., Mobley C. D., Steward R. G., Patch J. S., 1999, *Hyperspectral remote sensing for shallow waters: 2. Deriving bottom depths and water properties by optimization*, Appl. Opt., 38 (18), 3831–3843.
- Lee Z. P., Carder K. L., Steward R. G., Peacock T. G., Davis C. O., Patch J. S., 1998, *An empirical algorithm for light absorption by ocean water based on color*, J. Geophys. Res., 103 (C12), 27,967–27,978.
- Loisel H., Stramski D., Mitchell B. G., Fell F., Fournier-Sicre V., Lemasle B., Babin M., 2001, *Comparison of the ocean inherent optical properties obtained from measurements and inverse modeling*, Appl. Opt., 40 (15), 2384–2397.
- Lysiak-Pastuszak E., 2000, *An assessment of nutrient conditions in the southern Baltic Sea between 1994 and 1998*, Oceanologia, 42 (4), 425–448, ([www.iopan.gda.pl/oceanologia](http://www.iopan.gda.pl/oceanologia)).
- McCarthy M., Pratum T., Hedges J., Benner R., 1997, *Chemical composition of dissolved nitrogen in the ocean*, Nature, 390, 150–153.
- McClain C. R., Fargion G. S., 1999a, *SIMBIOS Project 1998 Annual Report*, NASA TM 1999–208645, Greenbelt, Maryland, Goddard Space Flight Centre, 128 pp.
- McClain C. R., Fargion G. S., 1999b, *SIMBIOS Project Annual Report*, NASA TM 1999–209486, Greenbelt, Maryland, Goddard Space Flight Centre, 128 pp.
- Mitchell B. G., Bricaud A., Carder K., Cleveland J., et al., 2000, *Determination of spectral absorption coefficients of particles, dissolved material and phytoplankton for discrete water samples*, [in:] *Ocean Optics Protocols for Satellite Ocean Color Sensor Validation. Revision 2*, G. S. Fargion & J. L. Mueller (eds.), NASA/TM–2000–209966, Greenbelt, Maryland, Goddard Space Flight Centre, 125–153.
- Mopper K., Feng Z., Bentjen S. B., Chen R. F., 1996, *Effects of cross-flow filtration on the absorption and fluorescence properties of seawater*, Mar. Chem., 55, 53–74.
- Moran M. A., Sheldon Jr W. M., Zepp R. G., 2000, *Carbon loss and optical property changes during long-term photochemical and biological degradation of estuarine dissolved organic matter*, Limnol. Oceanogr., 45 (6), 1254–1264.

- Mueller J. L., Austin R. W., 1995, *Ocean Optics Protocols for SeaWiFS Validation. Revision 1*, NASA TM-104566, Vol. 25, S. B. Hooker, E. R. Firestone & J. G. Acker (eds.), NASA Goddard Space Flight Centre, Greenbelt, Maryland, 67 pp.
- Neale P. J., Cullen J. J., Davis R. F., 1998, *Inhibition of marine photosynthesis by ultraviolet radiation: variable sensitivity of phytoplankton in the Weddell-Scotia Confluence during the austral spring*, *Limnol. Oceanogr.*, 43 (3), 433–448.
- Nelson N. B., Siegel D. A., Michaels A. F., 1998, *Seasonal dynamics of colored dissolved material in the Sargasso Sea*, *Deep-Sea Res. Pt I*, 45, 931–957.
- Nyquist G., 1979, *Investigation of some optical properties of sea water with special reference to lignin sulfonates and humic substances*, PhD Thesis, Dept. Analytical and Marine Chemistry, Göteborg University, Göteborg, Sweden, 203 pp.
- Okami N., Kishino M., Sugihara S., Takematsu N., Unoki S., 1982, *Analysis of Ocean Color Spectra (III) – Measurements of Optical Properties of Sea Water*, *J. Oceanogr. Soc. Jap.*, 38, 362–372.
- O'Reilly J. E., Maritorea S., Mitchell B. G., Siegel D. A., Carder K. L., Garver S. A., Kahru M., McClain C., 1998, *Ocean color chlorophyll algorithms for SeaWiFS*, *J. Geophys. Res.*, 103 (C11), 24,937–24,953.
- Pages J., Gadel F., 1990, *Dissolved organic matter and UV absorption in a tropical hyperhaline estuary*, *Sci. Total Environm.*, 99, 173–204.
- Patel N., Mounier S., Guyot J. L., Benamou C., Benaim J. Y., 1999, *Fluxes of dissolved and colloidal organic carbon, along the Purus and Amazonas rivers (Brazil)*, *Sci. Total Environm.*, 229, 53–64.
- Pegau W. S., Zaneveld J. R. V., Barnard A. H., Maske H., Alvarez-Borrego S., Lara-Lara R., Cervantes-Duarte R., 1999, *Inherent optical properties in the Gulf of California*, *Cienc. Mar.*, 25 (4), 469–485.
- Pempkowiak J., 1988, *The distribution, origin and properties of humic acids in the Baltic Sea*, Ossolineum, Wrocław, 146 pp., (in Polish).
- Raymond P. A., Bauer J. E., 2001, *Use of  $^{14}\text{C}$  and  $^{13}\text{C}$  natural abundances for evaluating riverine, estuarine and coastal DOC and POC sources and cycling: a review and synthesis*, *Org. Geochem.*, 32, 469–485.
- Reynolds R. A., Stramski D., Mitchell B. G., 2001, *A chlorophyll-dependent semianalytical reflectance model derived from field measurements of absorption and backscattering coefficients within the Southern Ocean*, *J. Geophys. Res.-Oceans*, 106 (C4), 7125–7138.
- Rozan T. F., Luther III G. W., 2002, *An anion chromatography/ultraviolet detection method to determine nitrite, nitrate and sulfide concentrations in saline (pore) waters*, *Mar. Chem.*, 77, 1–6.
- Schiller H., Doerffer R., 1999, *Neural network for emulation of an inverse model – operational derivation of Case II water properties from MERIS data*, *Int. J. Remote Sens.*, 20 (9), 1735–1746.

- Siegel H., Gerth M., Neumann T., Doerffer R., 1999, *Case studies on phytoplankton blooms in coastal and open waters of the Baltic Sea using Coastal Zone Color Scanner data*, Int. J. Remote Sens., 20 (7), 1249–1264.
- Smith R. C., Baker K. S., 1981, *Optical properties of the clearest natural waters*, Appl. Opt., 20, 177–184.
- Spitzky A., Ittekkot V., 1986, *Gelbstoff: an uncharacterized fraction of dissolved organic carbon*, [in:] *The influence of yellow substances on remote sensing of sea-water constituents from space, vol. II: Appendices*, GKSS Res. Centre Geesthacht, ESA Contract No. RFQ 3–5060/84/NL/MD, December 1986.
- Stewart A. J., Wetzel R. G., 1981, *Asymmetrical relationships between absorbance, fluorescence and dissolved organic carbon*, Limnol. Oceanogr., 26 (3), 590–597.
- Stramska M., Stramski D., Mitchell B. G., Mobley C. D., 2000, *Estimation of the absorption and backscattering coefficients from in-water radiometric measurements*, Limnol. Oceanogr., 45 (3), 628–641.
- Summers R. S., Roberts P. V., 1988, *Activated carbon adsorption of humic substances: 1. Heterodisperse mixtures and desorption*, J. Colloid Interface Sci., 122 (2), 367–381.
- Tassan S., 1994, *Local algorithms using SeaWiFS data for the retrieval of phytoplankton, pigments, suspended sediment and yellow substance in coastal waters*, Appl. Opt., 33 (12), 2369–2378.
- Thingstad T. F., Hagström Å., Rassoulzadegan F., 1997, *Accumulation of degradable DOC in surface waters: is it caused by a malfunctioning microbial loop?*, Limnol. Oceanogr., 42 (2), 398–404.
- Twardowski M. S., Donaghay P. L., 2001, *Separating in situ and terrigenous sources of absorption by dissolved materials in coastal waters*, J. Geophys. Res., 106 (C2), 2545–2560.
- Twardowski M. S., Sullivan J. M., Donaghay P. L., Zaneveld J. R. V., 1999, *Microscale quantification of the absorption by dissolved and particulate material in coastal waters with an AC-9*, J. Atmos. Ocean. Technol., 16 (6), 691–707.
- Warnock R. E., Gieskes W. W. C., van Laar S., 1999, *Regional and seasonal differences in light absorption by yellow substance in the Southern Bight of the North Sea*, J. Sea Res., 42, 169–178.
- Werdell P. J., Bailey S., Fargion G. S., 2000, *SeaBASS data protocols and policy*, [in:] *Ocean Optics Protocols for Ocean Color Sensor Validation. Revision 2*, NASA TM 2000–209966, Greenbelt, Maryland, NASA Goddard Space Flight Centre, 170–172.
- Woźniak B., 1995, *Absorption of radiation by components of sea water*, [in:] *Light in the sea: the primary interaction*, J. Dera & A. Zieliński, Rep. Inst. Oceanol. PAN, Sopot, (in Polish).
- Zweifel U. L., 1999, *Factors controlling accumulation of labile dissolved organic carbon in the Gulf of Riga*, Estuar. Coast. Shelf Sci., 48, 357–370.

## Appendix

**Notation & Abbreviations**

$A(\lambda)$	Absorbance
$a_g(\lambda)$	Absorption by CDOM [ $\text{m}^{-1}$ ]
CDOM	Coloured dissolved organic matter
DOC	Dissolved organic carbon
DOM	Dissolved organic matter
E	Energy [eV]
MW	Molecular weight
HDOM	High molecular weight dissolved organic matter
HMW	High molecular weight
LMW	Low molecular weight
GF/F	Glass fibre filter, Whatmann grade F (nominal pore size 0.7 $\mu\text{m}$ )
GF/C	Glass fibre filter, Whatmann grade C
HPLC	High performance liquid chromatography
POM	Particulate organic matter
$s$	Slope of the semilogarithmic CDOM absorption curve at an arbitrary wavelength [ $\text{nm}^{-1}$ ]
$s_{440}$	Slope of the semilogarithmic CDOM absorption curve over a minimum range of 400 to 440 nm [ $\text{nm}^{-1}$ ]
S	Salinity [PSU]
TSM	Total suspended matter
UV	Ultra-violet
VHDOM	Very high molecular weight dissolved organic matter